Effects of azimuth-symmetric acceptance cutoffs on the measured asymmetry in unpolarized Drell-Yan fixed-target experiments

EPJ manuscript No.
(will be inserted by the editor)

Effects of azimuth-symmetric acceptance cutoffs on the measured asymmetry in unpolarized Drell-Yan fixed target experiments

Acceptance cutoffs in Drell-Yan

A. Bianconi[1], M.P. Bussa[2], M. Destefanis[2], L. Ferrero[2], M. Greco[2], M. Maggiora[2], and S. Spataro[2]

[1] Dipartimento di Ingegneria dell'Informazione - Università degli Studi di Brescia, and Istituto Nazionale di Fisica Nucleare, Gruppo di Brescia, via Valotti 9, I-25123 Brescia, Italy
e-mail: bianconi@bs.infn.it

[2] Dipartimento di Fisica - Università degli Studi di Torino, Italy, and Istituto Nazionale di Fisica Nucleare, Sezione di Torino, via Giuria 1, I-10125 Torino, Italy

Abstract. Fixed-target unpolarized Drell-Yan experiments often feature an acceptance depending on the polar angle of the lepton tracks in the laboratory frame. Typically leptons are detected in a defined angular range, with a dead zone in the forward region. If the cutoffs imposed by the angular acceptance are independent of the azimuth, at first sight they do not appear dangerous for a measurement of the $cos(2\phi)$-asymmetry, relevant because of its association with the violation of the Lam-Tung rule and with the Boer-Mulders function. On the contrary, direct simulations show that up to 10 percent asymmetries are produced by these cutoffs. These artificial asymmetries present qualitative features that allow them to mimic the physical ones. They introduce some model-dependence in the measurements of the $cos(2\phi)$-asymmetry, since a precise reconstruction of the acceptance in the Collins-Soper frame requires a Monte Carlo simulation, that in turn requires some detailed physical input to generate event distributions. Although experiments in the eighties seem to have been aware of this problem, the possibility of using the Boer-Mulders function as an input parameter in the extraction of Transversity has much increased the requirements of precision on this measurement. Our simulations show that the safest approach to these measurements is a strong cutoff on the Collins-Soper polar angle. This reduces statistics, but does not necessarily decrease the precision in a measurement of the Boer-Mulders function.

PACS. 13.85.Qk Drell-Yan – 13.88.+e Polarization in interaction and scattering – 29.30.-h Spectrometers and spectroscopic techniques

1 Introduction

1.1 The physics case

Drell-Yan experiments[1] have a long history (a brief introduction may be found in chapter 5 of [2] and in the reviews[3] and [4], while an extensive data collection has been organized in the Hepdata database[5]. A more modern general scheme may be found in [6]).

One of the most interesting and controversial observables measured in unpolarized Drell-Yan is the so-called ν coefficient[7,8] associated with the $cos(2\phi)$ azimuthal asymmetry in the rest frame of the dilepton pair. This quantity has theoretical relevance because of its association with the violation of the PQCD Lam-Tung relation[7, 8], and with the T-odd Boer-Mulders distribution function[9, 10].

Recently, its relevance has been increased by the perspective of using it to extract transversity[11] from the combination of single-spin and unpolarized Drell-Yan measurements[This however requires the ν coefficient to be measured at an unprecedented level of precision: a result like $10\pm3\%$ in a measurement of the $cos(2\phi)$ asymmetry would be interesting in itself, but useless for a quantitative identification of transversity that may compete with other techniques.

This work is centered on the potential errors that a beam-related forward dead cone in the acceptance may introduce into a measurement of the $cos(2\phi)-$asymmetry. The subtle point is that an acceptance that does not depend on the azimuth in the laboratory frame is able to introduce azimuthal effects in the Collins-Soper frame[12] (or similar frames) where this asymmetry is measured. Distributions of the acceptance that depended on the azimuthal angle in the Collins-Soper frame were reported in works[13,14,15,16,17] presenting measurements of the $cos(2\phi)$ asymmetry in the years 1980-90. Here we use Monte Carlo simulations to analyze in detail and exten-

sively the effects of an azimuth-symmetric forward dead cone on the measured $cos(2\phi)$-asymmetry. We explore a range of beam energies going from 15 to 250 GeV, that is of interest for some proposals aimed at measuring the $cos(2\phi)$ asymmetry with high precision in the near future[18, 19,20,21,22].

1.2 General definitions

In this work we have used the following definitions:

- Laboratory frame: it is the frame where the target is at rest, with z axis along the beam direction.
- s is the squared center of mass energy per target nucleon. It is expressed in GeV^2/nucleon, and calculated as if the target consisted of one nucleon only.
- x_1 and x_2 are the longitudinal fractions of the annihilating partons: x_1 is from the projectile, and x_2 from the target (explicitly indicated as x_{target} in the figures).
- $q_\mu = (E_\gamma, \boldsymbol{q})$ is the 4-momentum of the virtual photon in the laboratory frame.
- $Q_T = \sqrt{q_x^2 + q_y^2}$ is the modulus of the transverse momentum of the virtual photon w.r.t. the beam axis.
- $Q = \sqrt{Q^2}$ is the "mass" of the virtual photon, or equivalently the invariant mass of the lepton pair, and in the following will be named "mass". Q is completely determined by s, x_1, x_2, Q_T. A standard approximation is $Q \approx x_1 x_2 s$, but this approximation gives the mass of the 4-vector $(Q_0, 0, 0, Q_z)$ and fails if Q_T is not much smaller than $x_1 x_2 s$, that is the rule in some of the below examined kinematics.
- θ and ϕ are the polar and azimuthal angles of *one* of the two leptons (since now on: the positive one) in a frame where the virtual photon is at rest and the leptons have opposite momenta. Although different choices exist for such a frame, here we will use the Collins-Soper frame[12].
- $\boldsymbol{q}^+$ and $\boldsymbol{q}^-$ are the lepton momenta in the laboratory frame, with $\boldsymbol{q}^+ + \boldsymbol{q}^- = \boldsymbol{q}$.
- θ_{Lab+} and θ_{Lab-} are the angles of the positive and negative muon in the laboratory frame, where the target is at rest and the z-axis is parallel to the momentum $\boldsymbol{P}_{beam}$. No term in the cross section depends on these angles, but in this work they are central because acceptance cutoffs are imposed on them.
- Collision plane: it is the plane, in the laboratory frame, containing $\boldsymbol{q}$ and the beam axis.
- Lepton plane: it is the plane, in the laboratory frame, containing the two lepton momenta (and $\boldsymbol{q}$).

The cross section for Drell-Yan dilepton production in scattering of unpolarized hadrons (charged pion, proton or antiproton vs a target nucleus) may be approximately written in the parton model form (see e.g. [2]):

$$\frac{d\sigma}{dx_1 dx_2 dQ_T d\Omega} \;=\; \frac{1}{s} \cdot W(x_1, x_2, Q_T) \cdot A(\theta, \phi). \qquad (1)$$

In unpolarized Drell-Yan, and far from kinematic regions where the virtual photon is dominated by quarkonium resonances, A has the form[7]:

$$A(\theta,\phi) \;=\; 1 \;+\; cos^2(\theta) \;+ \\ +\; \frac{\nu(s, x_1, x_2, Q_T)}{2} sin^2(\theta) cos(2\phi) \;+\; .... \qquad (2)$$

$W(x_1, x_2, Q_T)$ does not depend on the angles. $A(\theta, \phi)$ in principle depends on s, x_1, x_2, Q_T too.

The focus of the present work is on the $\nu cos(2\phi)$ term[7] present in $A(\theta, \phi)$. The idea is that an acceptance constraint $\theta_{Lab\pm} > \theta_{cutoff}$ produces an unphysical contribution to the $\nu cos(2\phi)$-term.

1.3 Collins-Soper frame and $cos(2\phi)$-asymmetry

Three relevant coordinate frames will be here considered: (1) The Laboratory frame, where the target is at rest, (2) the "Collider" frame, i.e. the center of mass frame of the projectile and of the hit nucleon, (3) the Collins-Soper frame.

The angular cutoff that is relevant in this work is imposed on the polar angle of each lepton in the Laboratory frame. The Collider frame is necessary as an intermediate step for calculating the longitudinal fractions and some auxiliary variables needed to define the Collins-Soper frame (for each event, we have a different Collins-Soper frame). The difference $\boldsymbol{p}_1 - \boldsymbol{p}_2$ of the 3-momenta of the colliding hadrons in the Collider frame identifies a direction, that is chosen as the z axis of the Collins-Soper frame. The momentum $\boldsymbol{q}^*$ of the virtual photon (of the dilepton pair) in the collider frame identifies the xz plane in the Collins-Soper frame. The angles θ and ϕ are the polar and the azimuthal angles of the positive lepton in this frame.

Some intuitive qualitative features of the Collins-Soper frame and of the $cos(2\phi)$ asymmetry are reported in the Discussion section. Both the lepton plane and the collision planes contain $\boldsymbol{q}$, and in most of the events (not in all) the angle that in the laboratory frame expresses the relative orientation of the lepton and collision planes around $\boldsymbol{q}$ is approximately the Collins-Soper azimuthal angle ϕ. In events with positive $cos(2\phi)$ the two planes are roughly parallel, as for the lepton pair A^+A^- in fig.1. In events with negative $cos(2\phi)$ the two planes are roughly perpendicular, as for the lepton pair B^+B^- in the same figure. There is no sensitivity to dipolar (lepton exchange) effects, since $cos(2\phi) \rightarrow cos(2\phi + 2\pi)$ when the two leptons are exchanged.

1.4 Acceptance on single muons, and on muon pairs

In a fixed target Drell-Yan experiment it is common to have a dead forward cone in the laboratory, and often a dead backward cone, where lepton tracks are invisible or submerged by noise. In other words, it is quite normal to have the acceptance limits $\theta_{forward} < \theta_{Lab\pm} < \theta_{backward}$. In the forward direction, the cone occupied by the beam

and by the diffraction products of the hadron collisions is a zero acceptance region. For a beam energy of magnitude 100 GeV this normally means a few degrees, decreasing at increasing beam energy.

Although both a forward and a backward cutoff produce effects like the ones discussed in the following, in this work we will limit the discussion to the effects of a forward cutoff. We will also restrict to the s range 30-500 GeV^2. This region includes the available measurements[13,14,15, 16,17] of a nonzero value for ν[1], and some proposals for measuring it in the near future[18,19,20,21,22].

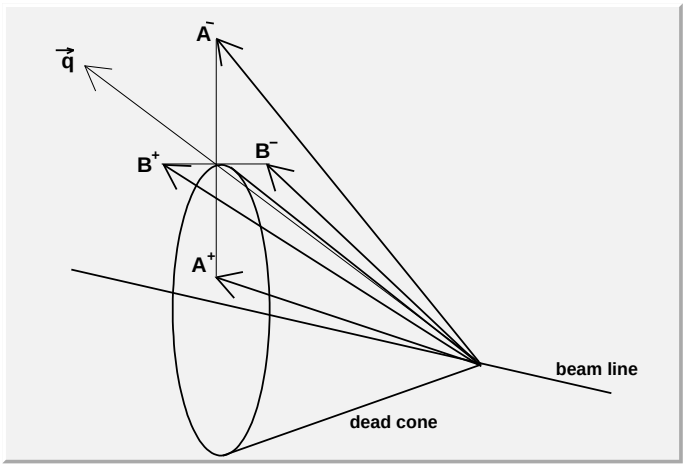

Fig. 1. Schematic representation of the described effect. A^+ and A^- are the tracks of a lepton pair composing an event where the lepton plane and the collision plane are parallel, while B^+ and B^- are the tracks of a lepton pair in an event where the lepton plane and the collision plane are perpendicular. For both events $\boldsymbol{q} = \boldsymbol{q}^+ + \boldsymbol{q}^-$ is the same and is tangent to the forward dead cone. Evidently, one of the four lepton tracks falls inside the dead cone (A^+), so that the A^+A^- event is not detected. The B^+B^- event is detected.

If the effect of a forward dead cone on single lepton tracks is evident, much more subtle is the effect it may have on lepton *pairs*. The key qualitative statement of this work is that a forward dead cone removes preferentially events where the lepton plane and the collision plane are parallel. This may be seen in the peculiar example shown in fig. 1.

The relevant elements appearing in this figure are:

1) a forward dead cone (with enlarged opening with respect to reality, for illustration purposes);

2) two possible lepton pairs (A^+A^- and B^+B^-) with the same $\boldsymbol{q} = \boldsymbol{q}^+ + \boldsymbol{q}^-$, but different space orientation for the lepton-antilepton plane;

3) $\boldsymbol{q}$ is chosen so to be tangent to the dead cone surface.

In the A^+A^- case one of the two leptons falls inside the dead cone. Since the pair is accepted only if two lepton tracks with opposite charge are detected, this pair is removed from the event collection of the experiment. In the B^+B^- case neither B^+ nor B^- is inside the dead cone, so this pair is detected and enters the event collection of the experiment. The A^+A^- pair has negative $cos(2\phi)$, the B^+B^- pair positive $cos(2\phi)$. All the other variables are equal for these two pairs. Therefore, by removing the former pair a false negative asymmetry is created.

Generalizing this example, a forward dead cone introduces a systematic anisotropy with respect to $cos(2\phi)$ into the distribution of the detected dilepton pairs. With suitable Monte Carlo simulations it is possible to study in a systematic way how large this effect can be.

1.5 Plan of this work

Section II is mainly devoted to the ways we have selected and organized the simulated data. Section III is developed around figures showing the simulation results: some examples of possible experiment output, dependence of the effects on the most important variables, interplay between physical and artificial effects. Section IV presents a discussion about the obtained results and the more general problems raised by such analysis.

2 Methods

2.1 Relevant kinematics

Two kinematic setups have special relevance in the following:

-) "**PANDA configuration**": antiproton projectile on a nuclear target (Z/A= 0.4), with

- the squared c.m. energy is s = 30 GeV^2/nucleon;
- the dilepton/virtual photon invariant mass Q satisfies 1.8 GeV $< Q <$ 2.7 GeV;
- the pair overall transverse momentum Q_T satisfies 0.5 GeV/c $< Q_T <$ 2 GeV/c.

In this configuration, inspired to the Drell-Yan program of the PANDA experiment[18,19], the relevant forward cutoff angles range from zero to about 10 degrees.

-) "**High-energy configuration**": negative pion projectile on a nuclear target (Z/A = 0.4), with

- the squared c.m. energy is s = 500 GeV^2/nucleon;
- the dilepton/virtual photon invariant mass Q satisfies 4 GeV $< Q <$ 8 GeV;
- the pair overall transverse momentum Q_T satisfies 1 GeV/c $< Q_T <$ 2.5 GeV/c.

In this configuration, inspired by past[2] and planned[3] pion-nucleus experiments, the relevant forward cutoff angles range from zero to about 1 degree.

We will mainly refer to events generated in the phase space associated to these two configurations, and to obvious modifications of them.

[1] More recently ν has been found compatible with zero by E866[23], but in a high-energy/small-x regime that makes this measurement peculiar. We will not care such situation here.

[2] The high-energy choice is close to the conditions of the experiments E615[17] (s = 474 GeV^2/nucleon) and NA10[15,16] running at its maximum beam energy (s = 537 GeV^2/nucleon).

[3] In the planned Drell-Yan at Compass-II[22] s ranges from 200 to 400 GeV^2/nucleon.

2.2 Asymmetry definitions

The asymmetry is here defined as in [24,25,26,27]. Let us assume that the phase space of the experiment is divided into bins associated to the values of variables like x, Q Q_T, θ, but excluding the azimuthal variable ϕ. So, the bin i contains events with ϕ spread over all the range $-180^o < \phi < 180^o$. Let us divide these events into two classes and define the **individual bin asymmetry**:

$$f_{i+} \leftrightarrow \cos(2\phi) > 0 \; in \; bin \; i \quad (3)$$

$$f_{i-} \leftrightarrow \cos(2\phi) < 0 \; in \; bin \; i \quad (4)$$

$$population_{(bin\ i)} = f_{i+} + f_{i-} \quad (5)$$

$$\mathbf{asymmetry_{(bin\ i)}} \equiv \frac{f_{i+} - f_{i-}}{f_{i+} + f_{i-}} \quad (6)$$

We also need the **full phase space integrated asymmetry**. This expression means that the complete phase space of the simulation (e.g. the phase space of the above described PANDA configuration) is divided into two halves corresponding to positive and negative values of $cos(2\phi)$.

Using this way for calculating the $\nu-$related asymmetry is especially simple, and in absence of any forward dead cone it would lead to measured asymmetries that are roughly $\approx \nu/2$. As it is evident from eq.2, ν coincides with $(f_+ - f_-)/(f_+ + f_-)$ when this quantity is estimated from a subset of events with $\theta \approx 90°$. To include the full phase space (or at least the region $|cos(\theta)| < 0.8$-0.9, as it was customary in past experiments) means to reduce the resulting asymmetry by about a factor 2, since $sin^2(\theta)$ reduces $f_+ - f_-$ while the factor $1+cos^2(\theta)$ increases $f_+ + f_-$ in eq.2.

2.3 Physical asymmetries

Some of our simulations refer to a hypothetical experiment where an azimuthal asymmetry is found and its origin is completely artificial. In other cases however, we will consider the combination of physical and artificial effects.

We will consider the possibility of a physical $cos(2\phi)$ asymmetry whose full phase space integrated values range between approximately -20 % and $+20$ %, analyzing the combined effect of this physical asymmetry and of an angular cutoff.

We also consider the effect of a physical $cos(\phi)$ asymmetry in affecting the relation between cutoff angles and false $cos(2\phi)$ asymmetries. We will not present the effects of the cutoffs on the measured $cos(\phi)$ asymmetry itself, because this would make the present work too much long.

The values of physical asymmetries employed in this work vary in ranges whose limits are $\pm$ 13.5 % for the $cos(2\phi)$ asymmetry, $\pm$ 16 % for the $cos(\phi)$ asymmetry in PANDA configuration, $\pm$ 22 % for the $cos(\phi)$ asymmetry in the high energy configuration. These values are "borderline" in the sense that with stronger asymmetries the Monte Carlo simulation meets negative value of the cross section somewhere at large Q_T.

2.4 Simulations: the generator code

The Monte Carlo simulation of Drell-Yan pairs is performed with the generator code[28] used in [24,25,26,27]. All details about the event generation technique may be found in these references. A critical discussion of the underlying formalism may be found in [29]. The cross section used for generating the events has the form given in eqs. 1 and 2, with the parameters tuned to those values that reproduce the results of the experiments [13,14,15,16,17] in the pion-nucleus case. For the antiproton-nucleus case the parameters of the cross section present a certain amount of modeling for lack of antiproton-nucleus data at the required center of mass energy.

2.5 Simulations: organization of the simulated events

In absence of angular cutoffs, the standard simulation used in this work produces 300,000 events. After applying acceptance cutoffs, the number N of events to be analyzed is in the range 120,000-300,000. These events have been treated in different ways:

- **Data Analysis Method 1**: The N events are considered as six independent simulations of an experiment that collects $N/6$ events. In each experiment the $N/6$ events may be further distributed into bins. The six repetitions of the simulation are treated as six independent experiments, and are exploited to estimate (i) the asymmetry measured in each bin as the average among the six values measured in each experiment for that bin, (ii) the error from an analysis of the fluctuations of the six measurements.
- **Data Analysis Method 2**: The simulated N events form a unique set, and the error in the asymmetry is estimated theoretically as $1/\sqrt{N}$ assuming a binomial distribution for the population of each of the two subsets a and b that we use to calculate the asymmetry as $(a-b)/(a+b)$.
- **Subset populations**: In some cases we have distributed the N events of a simulated sample into bins of some variable like x or Q_T. This strategy leads to bin populations and error bars that reproduce those of a real measurement. In the case of Q-binning over a wide Q-range we have preferred to produce an independent simulation for each Q-range, each with N events. This strategy was necessary to have reasonable error bars at large Q, without being obliged to produce huge numbers of events over the entire phase space. The relative size of the error bars at different Q does not reflect what would happen in a real experiment.

Method 1 is the one used in [24], where 50,000 events were identified as the minimum for a meaningful measurement of the relevant features of the $cos(2\phi)$ asymmetry as a function of x and Q_T, in a Q range of width 1-2 GeV above the applied threshold.

It was tested[24] that the average values and the errors were stable enough if the number of repetitions was

increased over six. However, the error estimated by this method is a random variable itself, and this is evident in some figures where nearby bins with very similar populations present different error bars.

Two kinds of error may be extracted this way. An average asymmetry calculated with Method 1 is the average of 6 asymmetries a_1, a_2, a_3, a_4, a_5, a_6: $a_{final} = (\sum a_i)/6$. Each a_i is extracted from $N/6$ events, so that a_{final} is approximately the asymmetry extracted from a set of N events[4].

The 1-σ-error δ extracted as $\delta^2 = \sum(a_i - a_{final})^2/5$ is an estimator for the error on *one* of the six values a_1, a_2, ...a_6. We will name this error "**individual experiment error**". On the other side, the error on the average of six identical measurements is $\sqrt{6}$ times smaller than the individual error. When we use $\delta_{final} = \delta_{final}/\sqrt{6}$ as an estimator for the error we write "**error on the theoretical estimate**".

In this work Method 2 has been applied to full phase space asymmetries, extracted from event samples with N ranging from 300,000 (no cuts) to 120,000 (the most severe cuts applied in this work, see later). The corresponding 1-σ error on the asymmetries is 0.002-0.003. This may be smaller than the errors of numeric origin (these may be estimated from irregularities in the presented curves). On the other side, the error in Method 1 is a combination of statistical and statistically distributed numeric errors, and for this reason is frequently larger than $1/\sqrt{N}$.

2.6 Forward angular cutoffs

In the following, the expression "applying a cutoff angle θ_{cutoff}" means that this event is excluded from the analyzed sample unless the individual lepton angles in the laboratory satisfy:

$$\theta_{Lab+} > \theta_{cutoff}, \quad (7)$$
$$\theta_{Lab-} > \theta_{cutoff}. \quad (8)$$

In absence of further specifications, in the present work "cutoff" means a cutoff applied to the polar angles in the laboratory frame.

3 Results

In all our simulations the fake asymmetry comes out to be negative. In the following, we have reproduced it as positive in all those figures where it appears alone and its sign has no role. When a fake and a true asymmetry are compared or mixed their relative sign has relevance. In these cases we have reproduced all the true and fake asymmetries with their proper sign.

[4] "Approximately" because an asymmetry $(a-b)/(a+b)$ is not linear in a and b, so the average of 6 asymmetries, each from 50,000 events, is not exactly the asymmetry from 300,000 events. For small asymmetries the approximation is precise.

3.1 Angular distribution of the events in the Collins-Soper frame

The angular distributions of the events in the Collins-Soper frame in presence of physical asymmetries and/or angular cutoffs are presented in figures 2 and 3.

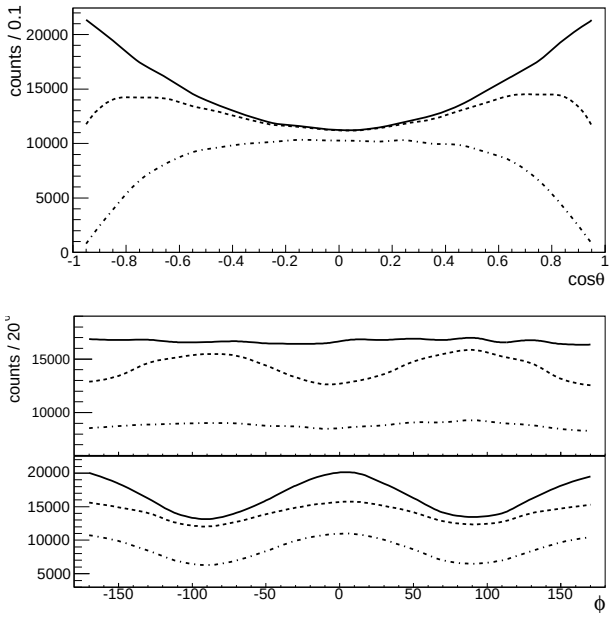

Fig. 2. Angular distributions in the Collins-Soper frame in PANDA configuration. In each panel, the continuous line corresponds to no cutoff, the dashed line to cutoff angles 5^o and the dash-dotted line to cutoff angle 10^o. Top panel: $cos(\theta)$ distributions, integrated w.r.t. ϕ. Bottom panel: ϕ distributions, integrated w.r.t. θ. Upper part of the bottom panel: no physical asymmetry. Lower part: physical asymmetry with full phase space value 16 %.

Fig.2 refers to PANDA configuration. In the upper panel we report the $cos(\theta)$-distribution of the events for cutoff angles 0^o, 5^o, 10^o. In absence of acceptance cutoffs the ϕ-integrated θ-distribution must follow the $1+cos^2(\theta)$ law expected from eq.2, since the other terms are removed by ϕ-integration. Therefore, the presence of a *physical* azimuthal asymmetry does not affect the $1 + cos^2(\theta)$ shape. On the contrary, the same panel shows that a forward cutoff in the laboratory removes events from the regions $\theta \approx 0^o$ and $\theta \approx 180^o$.

The lower panel is divided into two parts. In the upper part, we report the ϕ-distributions of the events for cutoff angles 0^o, 5^o, 10^o, in absence of any physical asymmetry effect. The no-cutoff curve is flat showing axial isotropy of the events in absence of a cutoff. For cutoff 5^o, we have the maximum $cos(2\phi)$-effect, i.e. a distribution with two peaks within the 2π-range. We notice that this artificial $cos(2\phi)$-term is negative. For cutoff 10^o the fake asymmetry is still present, but barely visible.

The lower part of the lower panel shows the effect of the same angular cutoffs 0^o, 5^o, 10^o in presence of a strong

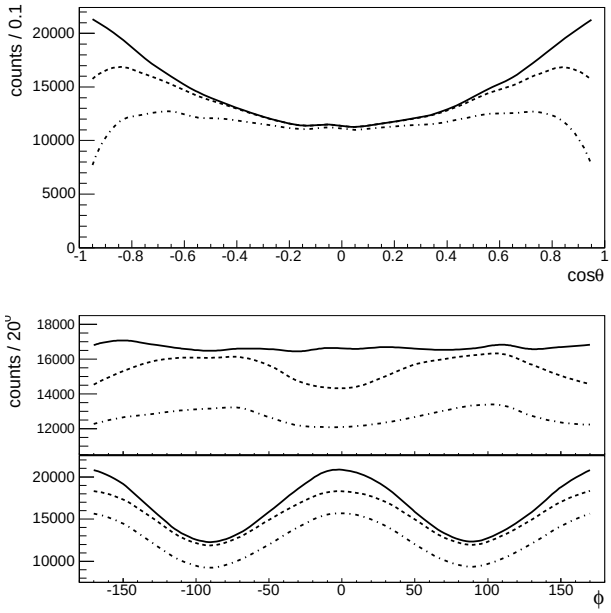

Fig. 3. Angular distributions in the Collins-Soper frame in high energy configuration. In each panel, the continuous line corresponds to no cutoff, the dashed line to cutoff angles 0.5^o and the dash-dotted line to cutoff angle 1^o. Top panel: $cos(\theta)$ distributions, integrated w.r.t. ϕ. Bottom panel: ϕ distributions, integrated w.r.t. θ. Upper part of the bottom panel: no physical asymmetry. Lower part: physical asymmetry with full phase space value 22 %.

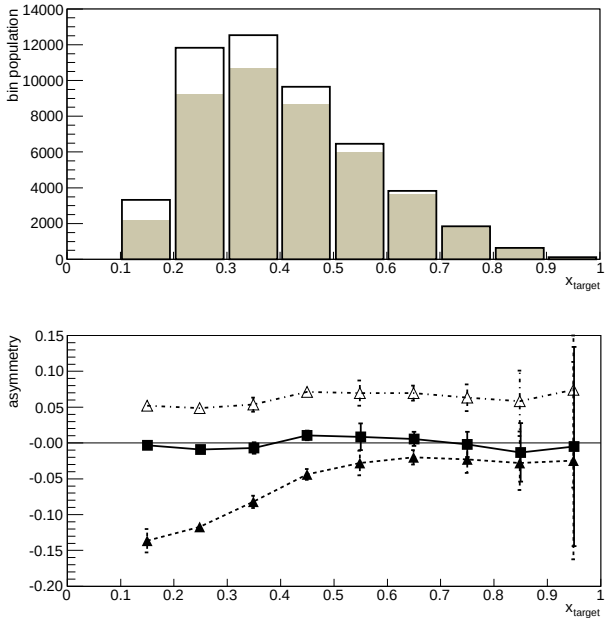

Fig. 4. Simulated experiment in PANDA configuration with Method 1. In the upper plot the bin population is shown for each x bin, without angular cutoff (black-line histogram) and with the cutoff $\theta_{lab\pm} > 5^\circ$ (shadowed histogram). In the lower plot, the extracted $cos(2\phi)$ asymmetry is shown. Continuous line: no physical asymmetry and no angular cutoff. Dot-dashed line: physical asymmetry with full phase space value 6.5 %, no angular cuts. Dashed line: no physical asymmetry, cutoff $\theta_{lab\pm} > 5^\circ$ cut. Error bars represent individual experiment errors.

physical asymmetry with positive sign (16 % full-phase-space integrated asymmetry). The two effects seem to interfere in a linear way, i.e. the sum of a large and positive physical asymmetry and of a smaller negative artificial asymmetry is a small positive asymmetry. The curve corresponding to cutoff 10^o is almost as flat as the no-cutoff curve, suggesting that at 10^o the fake asymmetry contribution is negligible.

The same analysis is reported in fig.3 for the high-energy configuration. In this case the cutoff angles are 0^o, 0.5^o, 1^o, and the full phase space physical asymmetry is 22 %. The qualitative conclusions are the same of the PANDA case.

3.2 Dependence of the fake asymmetry on the longitudinal fraction of the target

Here we adopt Method 1 of section 2.5 to simulate the outcome of an experiment in PANDA configuration (fig.4) and high-energy configuration (fig. 5). The events are divided into 10 bins of the target longitudinal fraction. In each bin the events are integrated over the longitudinal fraction of the projectile and all the other variables.

In both figures the event distributions with and without a forward cutoff are reported in the upper panel, the corresponding asymmetries in the lower panel. The curve close to zero values is the "reference" one, i.e. the corresponding simulations were performed with neither physical asymmetries nor angular cutoffs. Within the reported error bars, it coincides with zero everywhere.

In the PANDA configuration case (fig. 4) the positive-valued curve is a physical asymmetry with full-phase-space asymmetry 6.5 %, simulated in absence of any angular cutoff, according to the x-independent ν-distribution with the same Q_T-dependence as in [24]. The negative-valued curve is the fake asymmetry due to a forward angular cutoff 5^o.

In the high-energy configuration case (fig. 5) the positive-valued curve is a physical asymmetry with full-phase-space asymmetry 10 %, simulated in absence of any angular cutoff, according to the x-independent ν-distribution with the same Q_T-dependence as in [24]. The negative-valued curve is the fake asymmetry due to a forward angular cutoff 0.5^o.

3.3 Dependence of the fake asymmetry on the size of the angular cutoff

Here we use Method 1 to explore the dependence of the fake asymmetry on the size of the angular cutoff. No physical asymmetry is present. The results refer to the full phase space integrated asymmetry.

Fig. 6 refers to PANDA configuration. The applied cutoffs range from 0^o to 15^o.

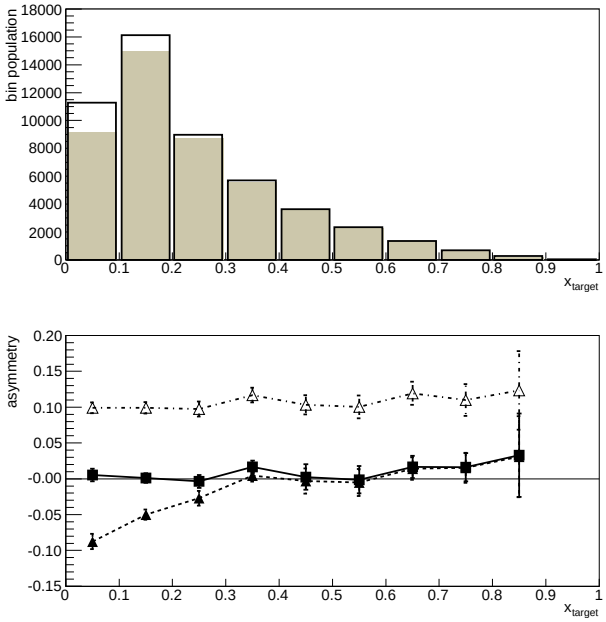

Fig. 5. Simulated experiment in high-energy configuration with Method 1. In the upper plot the bin population is shown for each x bin, without angular cutoff (black-line histogram) and with the cutoff $\theta_{lab\pm} > 0.5^\circ$ (shadowed histogram). In the lower plot, the extracted $cos(2\phi)$ asymmetry is shown. Continuous line: no physical asymmetry and no angular cutoff. Dot-dashed line: physical asymmetry with full phase space value 10 %, no angular cuts. Dashed line: no physical asymmetry, cutoff $\theta_{lab\pm} > 0.5^\circ$ cut. The error bars represent individual experiment errors.

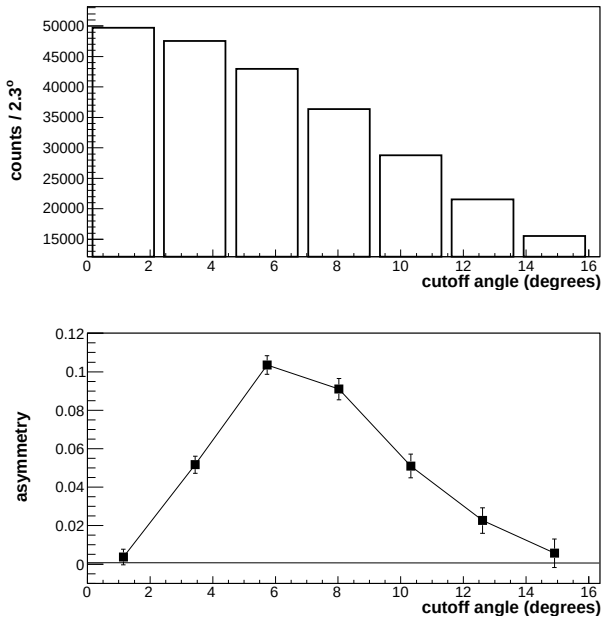

Fig. 6. Dependence of the fake asymmetry on the angular cutoff in PANDA configuration. Each point corresponds to a different forward cutoff angle. Upper panel: average event population after the forward angle cutoff has been applied. Lower panel: average overall asymmetry. Asymmetries and event numbers are extracted via Method 1. The error bars represent errors on the theoretical estimates.

Fig. 7 refers to the high energy configuration with restricted mass range 4.5 GeV $< Q <$ 5.5 GeV. The applied cutoffs range from zero to 1.5^o.

The biggest asymmetry is produced by angular cutoffs 6^o and 0.6^o for the two configurations respectively. These cutoff values will be used in the following to examine the dependence of the effect on transverse momentum, mass, and other cutoffs.

3.4 Dependence of the fake asymmetry on mass and transverse momentum

These dependencies are considered in the high-energy configuration scheme, where an experiment may collect events in a broad range of Q and Q_T. No physical asymmetry is included.

Fig.8 has been calculated in the restricted mass range 4.5 GeV $< Q <$ 5.5 GeV, with Method 1. The cutoff angle is 0.6^o, that according to fig.7 produces the maximum fake asymmetry effect in the high energy configuration.

Fig. 9 shows the dependence of the fake asymmetry effect on the virtual photon mass. Each mass bin has been treated as an independent experiment to which Method 1 has been applied, without sub-binning in any variable. The charmonium and bottonium regions have been excluded. Each curve in the figure corresponds to one value of forward cutoff: 0.6^o, 1.2^o, 1.8^o, 2.4^o.

3.5 Interaction with other cuts affecting the forward region

Typically in Drell-Yan experiments additional cutoffs in $x_F = x_1 - x_2$ and in $|cos(\theta)|$ are applied to the data. A cut on these parameters may remove lepton tracks from the forward region. In order to study its effect we have repeated the previous simulations imposing additional cutoffs on $|x_F|$ and in $|cos(\theta)|$.

The usual cut[13,14,15,16,17] $|x_F| < 0.9$ does not seem to introduce qualitative differences on the fake asymmetry. Stricter cuts on $|x_F|$ are not customary.

The effect of a cut on $|cos(\theta)|$ is more interesting, since limits $|cos(\theta)| < 0.8-0.9$ are the rule in Drell-Yan experiments to remove effects due to the rescattering in the nuclear target (see e.g. the discussion on the NA3 data analysis in [13]).

We show the combined effect of a laboratory forward cutoff and of a Collins-Soper polar cutoff in fig. 10. We work in the high-energy configuration. Two cutoffs are applied to the generated events:

a) A cutoff on the Collins-Soper angle θ:
$|cos(\theta)| < Max|cos(\theta)|$. Each point fig.10 corresponds to a different value of $Max|cos(\theta)|$.

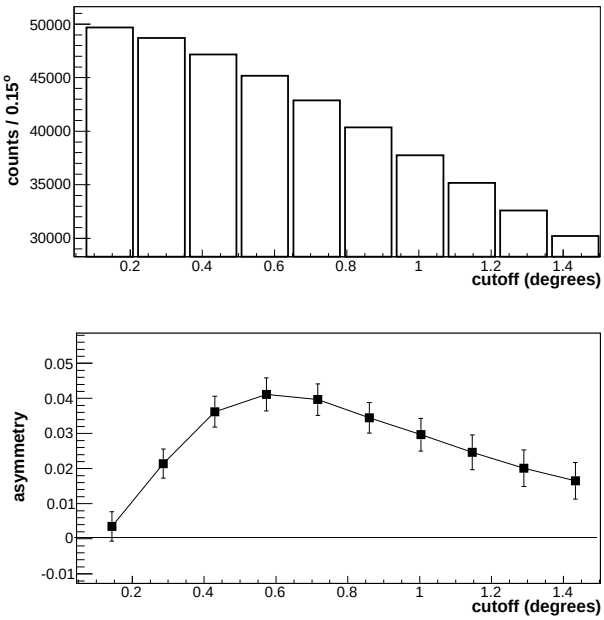

Fig. 7. Dependence of the false asymmetry on the angular cutoff, in high-energy configuration with the mass range restricted to $4.5 < Q < 5.5$ GeV. Each point corresponds to a different forward cutoff angle. Upper panel: average event population after the forward angle cutoff has been applied. Lower panel: average overall asymmetry. Asymmetries and event numbers are extracted via Method 1. The error bars represent errors on the theoretical estimates.

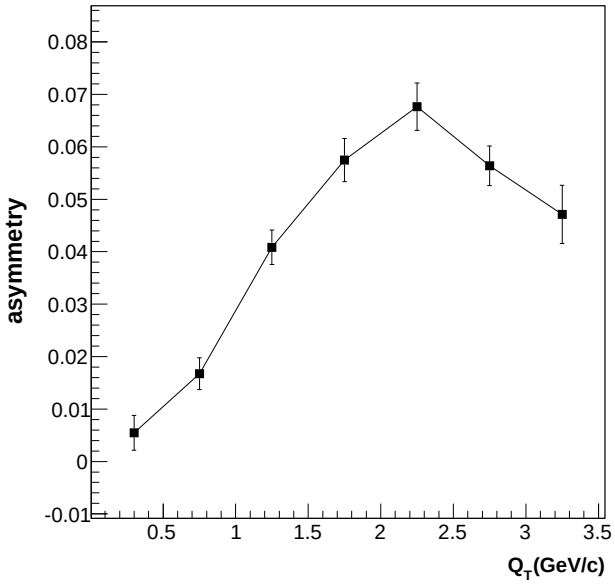

Fig. 8. Q_T-dependence of the false asymmetry in high-energy configuration, with the mass range restricted to $4.5 < Q < 5.5$ GeV. For all the points the angular cutoff is 0.6^o. These values have been extracted via Method 1. The error bars represent errors on the theoretical estimates.

b) A fixed cutoff $\theta_{Lab\pm} > 0.6^o$. This regards all the points in fig.10.

For each of the eight points reported in the figure an independent simulation according to method 1 is organized in the following way: The simulation generates exactly 6x50,000 events $after$ applying the cut (a), but $before$ imposing the cut (b). At this point, the application of cut (b) removes some extra events. The percentage of the extra events removed by cut (b) is reported in the upper panel of fig.10. Clearly, this percentage is large when no cut on the Collins-Soper polar angle has been applied. When a strong cut of this kind has been applied, the laboratory cut acts on events that have already been partially removed.

From the upper panel of fig.10 we see that after applying the cutoff $|cos(\theta)| < 0.7$ (equivalent to $50^o < \theta < 130^o$) the laboratory cutoff $\theta_{Lab\pm} > 0.6^o$ removes almost no events. This has the obvious consequence, visible in the lower panel, that the fake asymmetry reduces to zero in these conditions.

3.6 Interplay between true and fake asymmetries in presence of angular cutoffs

Another relevant point is the effect of an angular cutoff on a set of events where a true, physical azimuthal asymmetry is present. We have considered two possibilities:

(i) a set of data where a physical $cos(2\phi)$ asymmetry is present,

(ii) a set of data where a physical $cos(\phi)$ asymmetry is present.

Even the latter modifies the effect of the angular cutoff in producing an apparent $cos(2\phi)$ asymmetry[5].

The results discussed in this section are presented in figures 11, 12, 13, and 14.

They have been calculated with Method 2. The associated error on the estimated asymmetries is $1/\sqrt{N}$ and ranges from 0.002 to 0.003. In each figure of this section it is represented by a narrow band on the x-axis. We notice (see fig.13) that this error is smaller than the fluctuation between the values of the $cos(2\phi)$ asymmetry in absence of angular cutoffs but in presence of different $cos(\phi)$ asymmetry. Since this fluctuation is pure error, it signals that in these simulations the numeric error is as relevant as the statistic one, and an overall error of size 0.005 may be estimated.

We consider five different values of the physical $cos(2\phi)$ and $cos(\phi)$ asymmetries. Integrated over all the phase space, these are:

- $cos(2\phi)$ asymmetry in PANDA and high-energy configuration: 0, ± 6.5 %, ± 13.5 %.
- $cos(\phi)$ asymmetry in PANDA configuration: 0, ± 10 %, ± 16 %.

[5] We have not considered the effects of the angular cutoffs on the $cos(\phi)$ asymmetry itself because this is out of the main scope of this work.

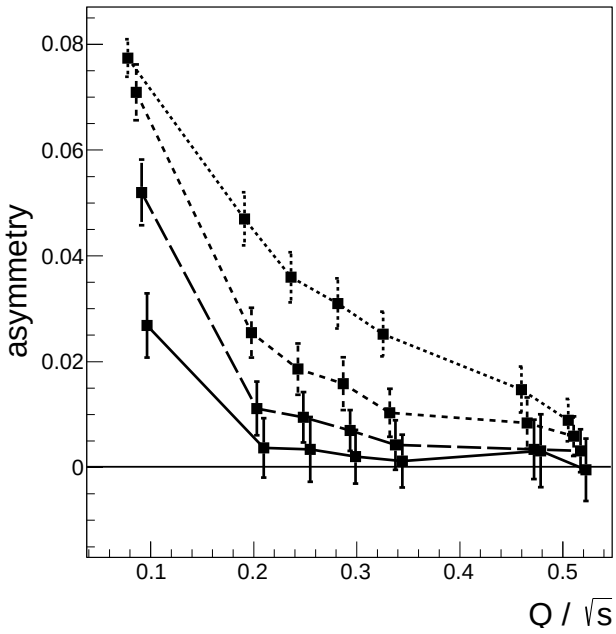

Fig. 9. Dependence of the fake asymmetry on the dilepton mass Q for several cutoffs in the laboratory angle, in high-energy configuration. Each curve corresponds to a different angular cutoff in the laboratory. Dotted curve: 0.6^o. Short-dashed curve: 1.2^o. Long-dashed curve: 1.8^o. Continuous curve: 2.4^o. For each curve, the presented points correspond to $Q-$ranges 1.5-2.5 GeV, 4-5 GeV, 5-6 GeV, 6-7 GeV, 7-8 GeV, 10-11 GeV, 11-12 GeV. For each mass range, the corresponding four points indicate the central value of the range, although we have slightly shifted them to avoid graphical overlap of the error bars. These values have been extracted via Method 1, independently applied to each Q-interval. The error bars represent errors on the theoretical estimates.

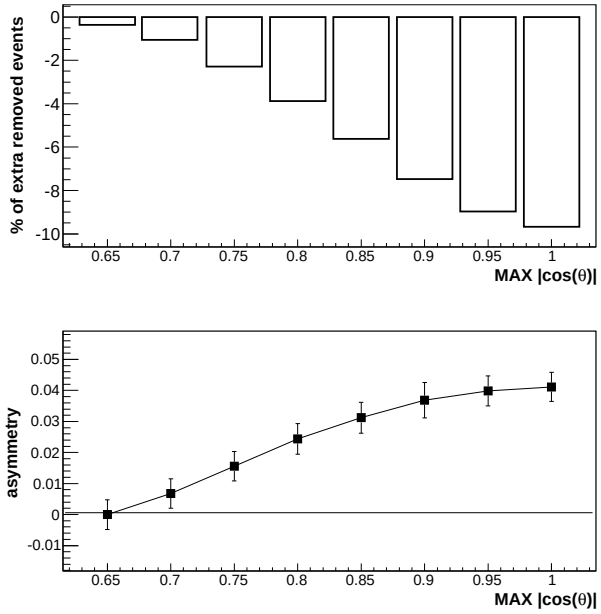

Fig. 10. Effect of an additional cutoff on the Collins-Soper polar angle θ in high-energy configuration. A fixed cutoff $\theta_{Lab\pm} > 0.6^o$ is present in all the points. A further cutoff is applied on the Collins-Soper angle θ: $|cos(\theta)| < Max|cos(\theta)|$. Each point corresponds to a different value of $Max|cos(\theta)|$. Upper panel: the percentage of the events removed by the laboratory cutoff after the cutoff on $|cos(\theta)|$ had been already applied. Lower panel: the fake asymmetry. These points have been reconstructed via Method 1. The error bars represent errors on the theoretical estimates.

– $cos(\phi)$ asymmetry in high-energy configuration: 0, ± 10 %, ± 22 %.

Each line in the figures 11 to 14 is associated to one of these values of physical asymmetry. A line shows how the measured $cos(2\phi)$ asymmetry changes at increasing angular cutoff.

The combined effects of a physical $cos(2\phi)$ asymmetry and of the angular cutoffs are reported in fig.11 (PANDA configuration) and fig.12 (high-energy configuration). These confirm the findings of figures 2, 3, 4, and 5, i.e. that a forward cutoff causes a fake contribution of negative sign to the measured asymmetry. Therefore, the angular cutoffs may enhance or decrease the absolute value of the measured asymmetry, depending on the sign of the true underlying asymmetry.

The joint effect of a nonzero physical $cos(\phi)$ asymmetry and of the angular cutoffs on the measured $cos(2\phi)$ asymmetry, in absence of a physical $cos(2\phi)$ asymmetry, is reported in fig.13 (PANDA configuration) and fig.14 (high-energy configuration).

As we see, for a given angular cutoff there is *some* dependence of the fake $cos(2\phi)$ asymmetry on the physical $cos(\phi)$ asymmetry. This dependence is however weak in the band ± 10 % of the physical asymmetry. If we compare figures 11 and 13 and observe the difference between the ± 10 % curves at 6^o where the cutoff-related distortion is maximum, this difference is over 12 % in fig. 11, but only 2.5 % in fig. 13. In the high energy configuration the difference between the two effects is even more marked (compare figures 12 and 14 at 0.6^o).

4 Discussion

4.1 Physical interpretation

Speaking in very approximate terms, the Collins-Soper frame, seen from the laboratory frame, has the z-axis parallel to the beam, and the x-axis parallel to $\boldsymbol{Q}_T$. What really modifies the forward angle of the physical momenta when passing from the laboratory frame to the Collins-Soper frame is the boost, since in the latter the virtual photon is at rest. Consequently:

– The angle θ is near 0^o when the positive muon is beam-parallel, near 180^o when the negative muon is beam-parallel. In these configurations the true $cos(2\phi)$ asymmetry is not present (see eq.2), while the forward cutoff has its maximum effectiveness.

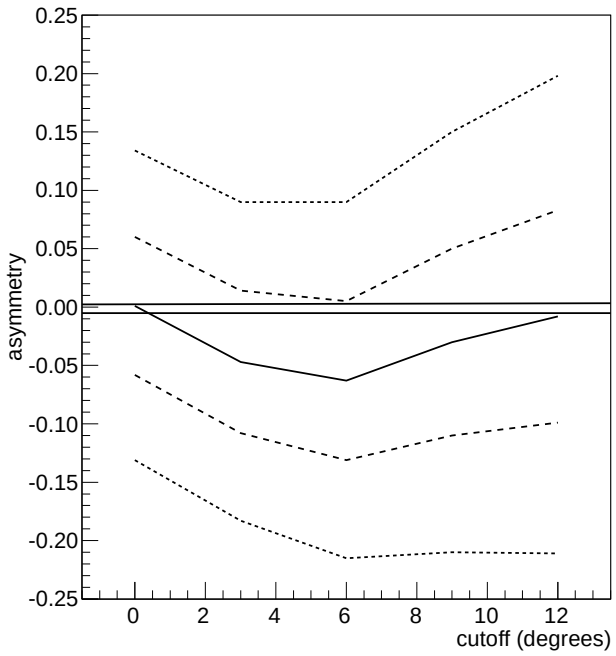

Fig. 11. Dependence of the overall (fake plus real) $cos(2\phi)-$asymmetry on the cutoff angle, for different values of $A_{true-2\phi}$, that is the real asymmetry integrated over all the phase space, in PANDA configuration. Continuous line: $A_{true-2\phi} = 0$. Long-dashed lines: $A_{true-2\phi} = \pm 0.065$. Short-dashed lines: $A_{true-2\phi} = \pm\ 0.135$. The continuous almost horizontal lines show the $\pm\sigma$ error band. These points have been extracted via Method 2.

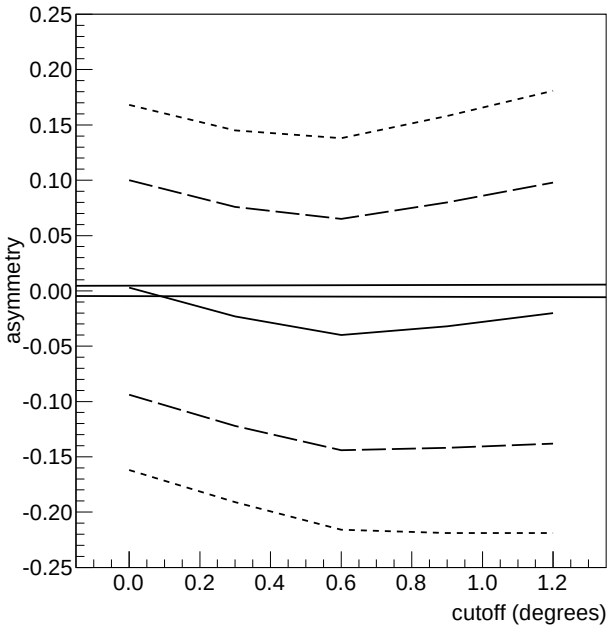

Fig. 12. Dependence of the overall (fake plus real) $cos(2\phi)-$asymmetry on the cutoff angle, for different values of $A_{true-2\phi}$, that is the real asymmetry integrated over all the phase space, in high energy configuration (see text). Continuous line: $A_{true-2\phi} = 0$. Long-dashed lines: $A_{true-2\phi} = \pm 0.065$. Short-dashed lines: $A_{true-2\phi} = \pm\ 0.135$. The continuous almost horizontal lines show the $\pm\sigma$ error band. These points have been extracted via Method 2.

- θ is near 90^o when the momenta q_+ and q_- of the muons in the laboratory have similar size, so that $\boldsymbol{q}_+ - \boldsymbol{q}_-$ is transverse. In these kinematics the physical $cos(2\phi)$ asymmetry is strong. The forward laboratory cutoff does not seem to be effective: the upper panels of figures 2 and 3 show that for $cos(\theta) \approx 0^o$ event frequencies are not decreased by the forward cutoff.
- ϕ roughly coincides with the angle between the transverse component of $\boldsymbol{q}_+ - \boldsymbol{q}_-$ and $\boldsymbol{Q}_T$ in the laboratory frame. In other words, with the angle between the lepton plane and the scattering plane (angle of rotation around the shared axis $\boldsymbol{q}$). A dominance of events where the transverse components of these two vectors are parallel or antiparallel means a positive $cos(2\phi)$ asymmetry. A dominance of events where they are orthogonal means a negative $cos(2\phi)$ asymmetry.

The fact that an artificial asymmetry is present means that there are configurations with fixed photon momentum, fixed $|\boldsymbol{q}_+|$, $|\boldsymbol{q}_-|$ and fixed angle α_{+-} between the two leptons, where a rotation of the lepton plane on the $\boldsymbol{q}$-axis transforms an accepted event into a rejected event or does the opposite. In other words, a rotation of the lepton plane on the $\boldsymbol{q}$-axis sends a muon track into the dead cone, or takes a muon track out of it. In absence of a physical $cos(2\phi)$ asymmetry, all the rotations of the lepton plane on the photon axis produce equally likely events. If some of these rotations lead to rejected events, they are not equally likely anymore.

In the situations examined in this work, the artificial asymmetry is always negative. Another way to describe the $cos(2\phi)$ asymmetry is that it is positive when one of the two muons is close to the beam axis and the other one is far, negative when their tracks have similar angles w.r.t. the beam. This explains the negative fake asymmetry suggesting that the events that are more frequently removed by a forward dead cone are those of the former kind, where one of the two tracks is dangerously close to the beam axis.

If the qualitative interpretation is simple, quantitative predictions are difficult. The fake asymmetry effect depends on the interplay between 3 angles in the laboratory: the cutoff angle, the virtual photon angle $\approx Q_T/Q_Z$, the angle α_{+-} between the two muons.

If one of these three angles is zero, the fake asymmetry is zero: it becomes impossible to imagine configurations where a rotation of the lepton plane on the $\boldsymbol{q}$-axis transforms an accepted event into a rejected event. If one angle is not exactly zero, but it is anyway much smaller than the other two, we may imagine configurations where a rotation of the lepton plane on the $\boldsymbol{q}$-axis transforms an accepted event into a rejected event, but these configurations are a small subset of the phase space.

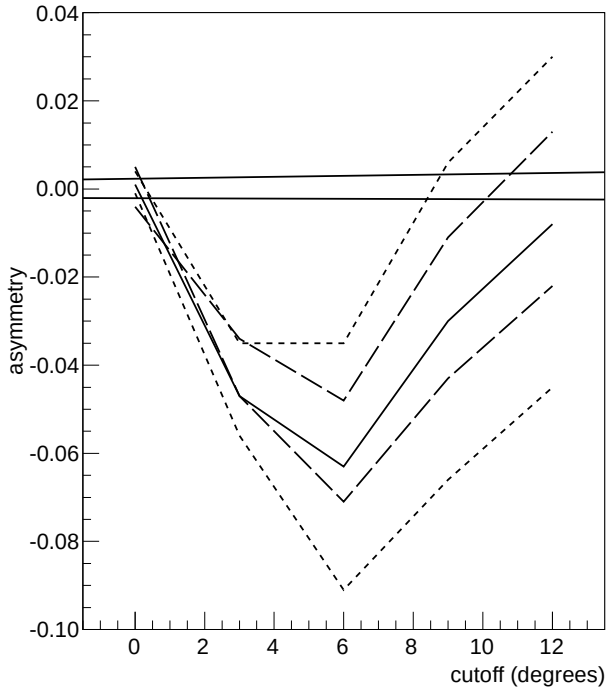

Fig. 13. Dependence of the overall (fake plus real) $cos(2\phi)-$asymmetry on the cutoff angle, for different values of $A_{true-\phi}$, that is the real $sin(2\theta)cos(\phi)-$asymmetry integrated over all the phase space, in PANDA configuration. Continuous line: $A_{true-\phi} = 0$. Long-dashed lines: $A_{true-\phi} = \pm 0.1$. Short-dashed lines: $A_{true-\phi} = \pm\ 0.16$. Going from negative to positive $A_{true-\phi}$, the reported curves become more negative. The continuous almost horizontal lines show the $\pm\sigma$ error band. These points have been extracted via Method 2.

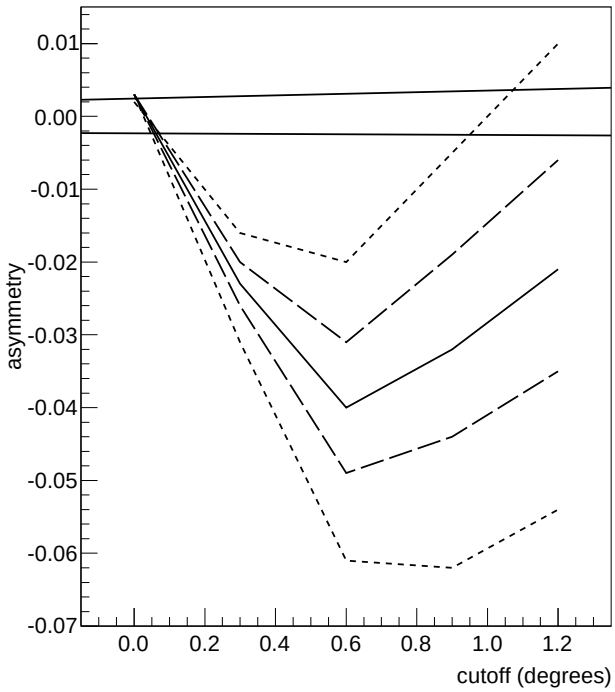

Fig. 14. Dependence of the overall (fake plus real) $cos(2\phi)-$asymmetry on the cutoff angle, for different values of $A_{true-\phi}$, that is the real $sin(2\theta)cos(\phi)-$asymmetry integrated over all the phase space, in high energy configuration. Continuous line: $A_{true-\phi} = 0$. Long-dashed lines: $A_{true-\phi} = \pm 0.1$. Short-dashed lines: $A_{true-\phi} = \pm\ 0.22$. Going from negative to positive $A_{true-\phi}$, the reported curves become more negative. The continuous almost horizontal lines show the $\pm\sigma$ error band. These points have been extracted via Method 2.

Something similar happens if one of the three angles is much larger than the other two. E.g., if the muon-muon angle is 10^o and the other two angles are 1^o, the minimum angle between one muon and the beam axis is 9^o that is out of the dead cone.

So, the fake asymmetry may be a statistically relevant effect at the condition that all these 3 angles have a similar magnitude. For a given cutoff angle, certain values of variables like Q, Q_T, or $x_{1,2}$ may statistically privilege values of the other two angles that are close each other, and close to the value of the cutoff angle.

Let us consider the high energy configuration, where kinematics allows for some approximations.

The virtual photon angle is Q_T/Q_Z. In the laboratory frame the energy of the virtual photon is mostly inherited by the beam parton, so $Q_Z \approx x_1 E_{beam} \approx x_1 s/2M_{nucleon} \approx x_1 \cdot 270$ GeV. In absence of asymmetric cuts in x_1 and x_2, the most frequent value for x_1 is given by the two equations $x_1 \approx x_2$, $x_1 x_2 = Q^2/s$, implying $x_1 \approx \sqrt{Q^2/s} \approx 0.23$ for $Q = 5$ GeV. A direct simulation confirms $< x_1 > = 0.23$.

This would lead to $Q_Z \approx 270 \cdot 0.23 \approx 60$ GeV. A direct simulation shows $Q_Z \approx 90$ GeV. In the high-energy configuration Q_T is constrained to the range 1-2.5 GeV/c and its simulated average value is 1.5 GeV/c, implying an angle $< Q_T > / < Q_Z > \approx 1.5/90$ that corresponds to 1^o. The direct average of the ratio $< Q_T/Q_Z >$ in the simulated data gives 1.35^o. In both cases the peak cutoff angle 0.6^o extracted from fig.7 is about 1/2 of the virtual photon angle.

In fig.8, where the cutoff angle is fixed while Q_T may freely assume any value in the range 0-3.5 GeV/c, the largest fake asymmetry effect is for Q_T = 2-2.5 GeV/c. The simulation, restricted to Q_T in the range 2-2.5 GeV/c, gives average photon angle 2^o, that is is more than 3 times the cutoff angle 0.6^o.

These distances between the cutoff angle and the photon angle may be justified observing in fig.5 that the fake asymmetry effect privileges small values of the target longitudinal fraction x_2, equivalent to large values of the projectile longitudinal fraction x_1 since $x_1 x_2 \approx Q^2/s$. This means that the relevant events present a virtual photon with Q_Z larger than the average 90 GeV/c. This means that we have photon angles that are smaller than their global average, in those kinematic regions of x_1 and x_2 where the fake asymmetry effect is built.

We know from the presented distributions that the fake asymmetry in the high-energy regime only regards 8 % of the events at most. These events are likely to be fluctuations (as a small x_2 suggests) where the photon angle is especially small.

It is more difficult to understand the role of the muon-muon angle α_{+-}. Roughly, the average angle $< \alpha_{+-} >$ between the two leptons in the laboratory is $\propto Q$, or to $\sqrt{x_2/x_1}$. Defining y as the fraction of photon energy taken by the positive muon, we have $E_+ \equiv yE_\gamma$, and $E_- \equiv (1-y)E_\gamma$, meaning $Q^2 \approx y(1-y)E_\gamma^2\alpha_{+-}^2$. Using $E_\gamma \approx Q_Z \approx x_1E_{beam} \approx x_1 s/2M_{nucleon}$ we get $x_2/x_1 \approx \alpha_{+-}^2 y(1-y)s/4M_{nucleon}^2$.

These approximations suggest that in fig.9 passing from $Q = 2$ GeV to $Q = 12$ GeV increases $< \alpha_{+-} >$ by six times, while in fig.5 increasing $x_{target} \equiv x_2$ means to increase $< \alpha_{+-} >$. Both operations cause the fake asymmetry effect to disappear.

For symmetry, the most likely value of the average $\sqrt{y(1-y)}$ is 0.5, and $s/4M_{nucleon}^2 \approx 140$. This gives $< \alpha_{+-} > \approx 7^o\sqrt{x_2/x_1}$ suggesting a typical angle 7^o. This may seem large, but a direct simulation in the mass range 4-8 GeV gave $< \alpha_{+-} > \approx 15^o$ (average on the sphere, i.e. over $cos(\alpha_{+-})$. Restricting the mass range to 4-5 GeV changes very little.

What gives such a large average value to this angle are relatively rare decays in which one muon is backward-directed in the Collins-Soper frame, so to have small energy and a very large angle in the laboratory: the average of nine 2^o angles plus one 180^o angle is 20^o.

The peak of the distribution of $cos(\alpha_{+-})$ is at 3.5^o. Whether one prefers to attribute relevance to 3.5^o, to 7^o or to 15^o is a matter of taste, but all of them are much larger than the cutoff angle and the photon angle.

However, reproducing the $cos(\alpha_{+-})$-distribution in the mass range 1.5-2.5 GeV shows that $< \alpha_{+-} >$ has more or less the same value as in the 4-8 GeV mass range, while the peak α_{+-} is now 1.5^o, not so far from the cutoff angle. The fact that at decreasing mass we have the same average angle, but a more forward peak in the distribution means that the population of the angles $< 1^o$ increases at decreasing masses.

Comparing this fact with the fast decrease of the fake asymmetry at increasing masses in fig.9, we have good reasons to guess that the fake asymmetry is due to the small-angle part of the distribution of α_{+-}, that is more populated at smaller Q. If we could extrapolate the Drell-Yan process to $Q < 15$ GeV[6] we would find a maximum of the fake effect, and a decrease of the effect at lower masses, or equivalently lower x_2 for a given x_1.

Summarizing this part, we expect to find a strong fake asymmetry effect when the cutoff angle, the virtual photon angle, and the lepton-lepton angle are similar. In the high energy configuration the average values of the virtual photon angle and of the lepton-lepton angle cannot realize this. Fluctuations from the averages of these two angles may combine so to do it, and this justifies the fact that the fake asymmetry is statistically a small effect, and that it is present at peculiar kinematics (e.g. small target x).

[6] that is not possible since the vector mesons dominate the cross section, so another physics has to be taken into account.

4.2 Perspectives

From fig. 10 it can be deduced that a strong $|cos(\theta)|$ cutoff assures a clean asymmetry measurement even without model-dependent Monte Carlo corrections. This fact is supported by the qualitative considerations at the beginning of the Discussion section. Removing broad angular regions implies the cost of a relevant reduction in the experiment statistics. However, in [24] it was shown by direct simulations and assuming a nonzero physical asymmetry, that the optimal compromise between statistics and asymmetry dilution is reached with a rather strong cutoff in the Collins-Soper frame, excluding events out of the range $60^o < \theta < 120^o$, i.e. requiring the cutoff $|cos(\theta)| < 0.5$. This cutoff is more restrictive than any cutoff reported in fig.10. The argument in [24] was that the physical $cos(2\phi)$ asymmetry is proportional to the factor $sin^2(\theta)$ in eq.2. As a consequence the removed events do not contribute to the asymmetry, but rather dilute it.

The fake asymmetries induced by cuts on the acceptance in the forward region feature a behavior that is similar in several respects to the one of the asymmetries measured in the experiments previously cited: both decrease at increasing $Q/\sqrt{s}$, both increase at increasing Q_T. The size of the fake asymmetry is smaller, but not by orders.

With more than 10,000 useful events, and in the same kinematic regime considered in this work (beam energies far below 1000 GeV), ν has been measured by the collaborations NA3[13,14], NA10[15,16], E615[17] in the decade 1980-90, leading to results that are similar in magnitude ($\nu \sim 0.1$ at $Q_T > 1$ GeV/c) and present similar qualitative behaviors, within error bars. Although the related papers quoted here do not present a complete description of all the technical details of the data analysis, some figures are present showing a non-flat acceptance as a function of ϕ in the Collins-Soper frame. Therefore, we can assume that all the acceptance problems have been implicitly considered.

Because of the limited phase space covered, in the NA10 experiment the $|cos(\theta)|$ maximum was set to 0.5 or 0.6, depending on the run (see [15,16]). This excluded the dangerous region of the forward angles. The corresponding fake asymmetry is negligible, as it may be deduced from fig. 10. The experiments NA3[13,14] and E615[17] put constraints on $cos(\theta)$ but not so severe. Their results are anyway similar to those from NA10.

The procedure adopted by NA10 and NA3, according to the quoted papers, was expressing the theoretical cross section in terms of a set of parameters, convoluting this with the experiment known acceptance, generating events and comparing their distribution with the experimental outcome to select a reliable set of parameters including ν. Although in some schemes the number of parameters may be as large as seven, it was remarked in [13] that the ν-parameter is constrained by the distribution of the events coming from a specific phase space region (θ near

90^o) where the other parameters related with the angular distribution have little influence. So the search of the optimal value of the ν-parameter was safer than the number of involved parameters could suggest. In the E615 case[17] the technique was to integrate over two of the three angular parameters, while looking for a functional form $\nu(Q_T, x, ...)$ for the third one that gave a satisfactory fit of the cross section behavior.

In perspective, we should notice that to obtain a relative error $\pm 15\%$ on a single ν value summarizing the Q-range 4-4.5 GeV, the NA10 experiment had to concentrate 40,000 events with $|cos(\theta)| < 0.6$ in that mass range. If these events were distributed in a finer $x-$binning, it would be difficult to reach a higher precision than $\pm 30\%$ in the most populated bins. This suggests that very careful planning, and large event numbers, are necessary to allow the precision on the ν-parameter to increase in magnitude w.r.t. the presently available values from the quoted experiments.

4.3 Conclusions

We have shown that a forward dead cone in the laboratory frame seriously affects a measurement of a Lam-Tung-style lepton asymmetry. This could be a problem for experiments aiming at reducing the relative errors on the ν-parameter to less than 20 % in a broad x-range, in particular when the values of this parameter are needed as an input to extract Transversity from a single-spin Drell-Yan experiment.

Our results show that the fake asymmetry is relevant for special values of the forward cutoff angle. Approximately, these correspond to situations where the cutoff angle, the polar angle and the angle betwen the two leptons have similar magnitudes in the laboratory.

Fig.10 suggests that restricting the data analysis to regions near $\theta = 90^o$ should be the safest way to obtain a result that is model-independent and precise. This agrees with the suggestion given in [24], that including events from θ-regions far from 90^o does not improve the quality of a measurement of the physical $cos(2\phi)$ asymmetry.

References

1. S.D.Drell and T.M.Yan, Phys. Rev. Lett. **25** (1970) 316.
2. R.D.Field, "Applications of Perturbative QCD", Addison-Wesley Publishing Company, 1989.
3. G.Matthiae, Riv. Nuovo Cim. 4N3:1-58 (1981).
4. I.R.Kenyon, Rep.Progr.Phys. **45** 1261 (1982).
5. HEPDATA: the Durham HEP Database, cared by the Durham Database Group of the Durham University (UK). http://durpdg.dur.ac.uk/
6. S. Arnold, A. Metz, and M. Schlegel, Phys.Rev.**D79**, 034005 (2009);
7. C.S.Lam and W.-K.Tung, Phys.Rev. **D 18** 2447.
8. C.S.Lam and W.-K.Tung, Phys.Rev. **D 21** 2712.
9. D.Boer and P.J.Mulders, Phys.Rev. **D57**, 5780 (1998).
10. D.Boer, PRD 60 (1999) 014012.
11. J.P.Ralston and D.E.Soper, Nucl.Phys.**B 152**, 109 (1979).
12. J.C.Collins and D.E.Soper, Phys. Rev. **D 16** (1977) 2219.
13. J.Badier et al, Z.Phys.**C 11** 195 (1981);
14. O.Callot, preprint LAL-81-08 mar 81 (available at the KEK online preprint library), published in the Proceedings of the 1st Moriond Workshop, Les Arcs, France, 25-30 Jan 1981, ed. J.Tran Thanh Van, Frontieres 1981.
15. S.Falciano et al, Z.Phys.**C 31** 513 (1986);
16. M.Guanziroli et al, Z.Phys.**C 37** 545 (1988).
17. Conway et al, Phys.Rev.**D 39** (1989) 92.
18. PANDA collaboration, L.o.I. for the *Proton-Antiproton Darmstadt Experiment* (2004), `http://www.gsi.de/documents/DOC-2004-Jan-115-1.pdf`.
19. W.Erni et al, "Physics Performance Report for PANDA: Strong Interaction Studies with Antiprotons", arXiv 0903.3905.
20. P. Lenisa and F. Rathmann [for the PAX collaboration], hep-ex/0505054.
21. M.Maggiora (for the ASSIA collaboration), "Spin physics with antiprotons", preceedings of "Spin and Symmetry" conference, Prague 2005, Czech.J.Phys. 55, A75 (2005).
22. E.Gautheron et al, "Compass-II Proposal", CERNSPSC2010014, SPSC-P-340, may 17, 2010. Freely available at http://wwwcompass.cern.ch/compass/proposal/compass-II_proposal
23. L.Y.Zhu et al, Phys.Rev.Lett.**99** 082301 (2007).
24. A.Bianconi and M.Radici, Phys.Rev. **D 71** (2005) 074014.
25. A.Bianconi and M.Radici, Phys.Rev. **D 72** (2005) 074013.
26. A.Bianconi and M.Radici, Phys.Rev. **D 73** (2006) 034018.
27. A.Bianconi and M.Radici, Phys.Rev. **D 73** (2006) 114002.
28. A.Bianconi, Nuclear Inst. and Methods in Physics Research, **A 593** 562 (2008).
29. A.Bianconi and M.Radici, J. Phys. G: Nucl. Part. Phys. 34 No 7 (July 2007) 1595